

Optical and ESR study of Er^{3+} in LiNbO_3

D.M.B.P. Milori, I.J. Moraes,* A.C. Hernandez, R.R. de Souza, M. Siu Li, and M.C. Terrile
*Instituto de Física de São Carlos, Universidade de São Paulo-São Carlos, Caixa Postal 369,
 13560 São Carlos, São Paulo, Brazil*

G.E. Barberis

Instituto de Física "Gleb Wataghin," Universidade Estadual de Campinas, 13083-970 Campinas, São Paulo, Brazil
 (Received 1 July 1994)

We report laser-excited optical transitions between the $^4S_{3/2}$ and $^4I_{15/2}$ multiplets of Er^{3+} as an impurity in the LiNbO_3 host, together with the optical-absorption spectra at liquid-helium and liquid-nitrogen temperatures. The optical data allow us to determine the crystal-field splittings of those levels and the spin-Hamiltonian parameters for the $^4I_{15/2}$ lower multiplet. The observed electron-spin resonance and the angular variation of this spectrum agree with the parameters obtained by optical techniques. Both techniques show that only one of the three possible trigonal sites in LiNbO_3 is occupied by Er^{3+} within the experimental sensitivity, in agreement with recent x-ray standing-wave measurements.

I. INTRODUCTION

Much interest in studying LiNbO_3 by physical methods has recently arisen, due to the unique physical properties presented by this ferroelectric material, such as photovoltaic, piezoelectric, elasto-optic, and photorefractive effects. Some of these properties are drastically affected by the presence of impurities, growing conditions, or thermal treatment, thus determining or affecting the particular technical application for the material. A large amount of papers has been published on this subject in the last decade, particularly oriented to the use of LiNbO_3 as a laser active medium, and monolithic integration of active electro-optic devices within the laser material.¹⁻⁷ The development of Er^{3+} amplifiers in optical fibers, and the great improvement that this gave to communications, have increased the research in materials such as $\text{LiNbO}_3:\text{Er}^{3+}$ that could be used as an active medium for the Er^{3+} frequencies.

Electron-spin resonance (ESR) studies of other rare-earth and $3d$ ions in LiNbO_3 (Gd^{3+} , Yb^{3+} , Nd^{3+} , Fe^{3+} , and Cr^{3+}) (Refs. 2, 3) show trigonal symmetry, as expected from magnetic ions substituting for Li or Nb in the lattice, or located as interstitial ions in the most probable position of the unit cell. One of the existing examples² shows that two different sites were found for Gd^{3+} in LiNbO_3 , but our ESR experiments and the optical data here presented show only one unique site for the Er^{3+} ion in LiNbO_3 within the experimental error. Very recently, Gog *et al.*,⁴ using the x-ray standing-wave (XSW) technique, determined that the site occupied by Er^{3+} is a position near the Li site, with the same trigonal symmetry, displaced slightly in the $-c$ axis direction. They used nearly perfect single crystals, with Er^{3+} introduced by diffusion, in very small concentrations. Our work corroborates the statement made in Ref. 4, in the sense that only one trigonal site is occupied by the rare earth.

II. EXPERIMENTAL DETAILS

The samples used in our experiments were grown by the Czochralski method, using an automatic crystal growth system from Cambridge Instruments. They were prepared by melting optically pure Li_2CO_3 and Nb_2O_5 in the correct congruent proportions obtained from the phase diagram (48.6% of the first and 51.4% of the second). Seeds were oriented with the c axis in the vertical direction, to obtain oriented single crystals. Er_2O_3 was diluted in the melt to obtain Er^{3+} as impurity. The nominal Er concentration was 0.05 mol% in all our samples. As the fusion temperature of the melt (1253 °C) is higher than the ferroelectric critical temperature ($T_c \approx 1210$ °C) the crystals grow in the paraelectric phase, giving origin to multidomains as they are cooled, with their optical and magnetic characteristics altered. To avoid that, we applied a small electric field to the melt during the growing ($|\vec{E}| = 0.2$ V/cm, corresponding to a current of 1.2 mA/cm²) obtaining single domain single crystals. As Fe and the ions OH^- are natural impurities in the samples, we did a study of annealing methods, oriented to purify the samples. After shaping and polishing the samples thoroughly, we annealed them in an oxygen atmosphere, in a ceramic crucible at 700 °C, for eight hours. The resulting samples are perfectly transparent, and neither the ESR nor the optical measurements show the presence of Fe. OH^- ions were not detected by optical means, either.

The fluorescence spectrum was obtained by exciting the samples with an argon-ion laser using the 4880 and 4765 Å lines at room temperature and liquid nitrogen in a classical experimental arrangement. We used a 0.5 m Jarrel-Ash 82-000 monochromator, and a Thorn Emi 9558 QA photomultiplier as detector.

Polarized absorption experiments in the range from 33 330 to 5000 cm^{-1} were done with a Cary-17 spectrophotometer with a Glan-Thompson calcite polarizer.

From 4000 to 200 cm^{-1} , a Perkin-Elmer 180 was employed. The minimum spectral resolution was 1 cm^{-1} . The cooling of the samples was obtained by immersion.

The ESR measurements were carried out with an X-band Varian E-109 spectrometer, using 100 kHz magnetic field modulation. The power applied to the samples was 10 mW in most of the experiments. We cooled the samples with an APD Cryogenics Inc. model LTR-3 Helitran, adapted to the microwave cavity. We used liquid helium as cryogenic liquid.

III. RESULTS AND DISCUSSION

The LiNbO_3 crystal belongs to the C_{3v}^6 ($R3c$) space group, where Li^+ is in the $[0,0,1/4]$ position, and Nb^{5+} in the $[0,0,0]$, both in the trigonal axis. Cationic impurities enter into the lattice by substituting for those ions, or in an interstitial position also belonging to the c axis $[0,0,1/6]$. Always, the point symmetry of the impurity is C_3 , and it produces an angular variation of the ESR spectra that is axial in every case. Group theory can be used to predict the optical and electron paramagnetic resonance (EPR) spectra. As is known, for the C_3 point group, the lower $^4I_{15/2}$ multiplet of Er^{3+} splits completely into eight Kramers doublets.

Figure 1 shows partially the experimental fluorescence spectra of Er^{3+} in LiNbO_3 , where the so-called π (parallel to the ferroelectric axis) and σ (perpendicular to it) polarizations of the light are indicated with dashed and full lines, respectively. The numbering of the peaks identifies the transitions between the $^4S_{3/2} \rightarrow ^4I_{15/2}$ Er^{3+} multiplets. Figure 2 shows the absorption spectra obtained at liquid-helium temperature, where only the lowest level of the Er^{3+} ion is highly populated. Only two peaks can be seen, with different intensities for each of the polarization directions. Figure 3 shows the absorption spectra at

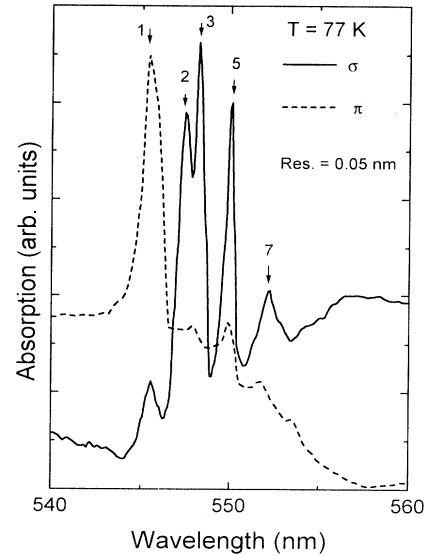


FIG. 2. Absorption spectra of $\text{LiNbO}_3:\text{Er}^{3+}$ at liquid-helium temperature for both polarization directions. The peaks are numbered in accordance with Fig. 4 below.

liquid-nitrogen temperature, where other than the lowest level of the $^4I_{15/2}$ multiplet are populated: several peaks, numbered to be identified, can be seen for both polarization directions in the same wavelength region. Figure 4 summarizes the level diagram obtained from the optical spectra together with the levels calculated by fitting the Hamiltonian

$$\hat{H}_{cc} = \frac{B_2^0}{\sqrt{3}}[O_2^1(c) + O_2^1(s) + O_2^2(s)] + B_2O_2^0 + B_4O_4 + B_6O_6 \quad (1)$$

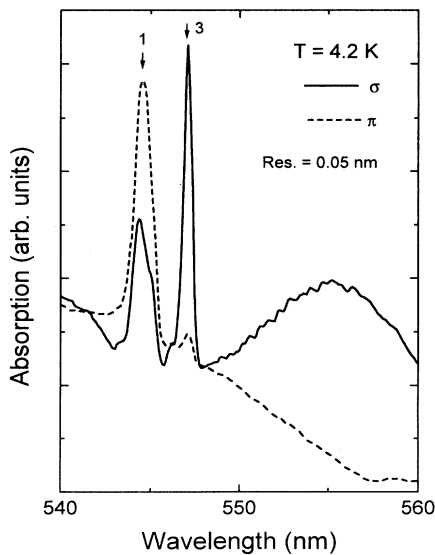


FIG. 1. Fluorescence spectra of $\text{LiNbO}_3:\text{Er}^{3+}$ where the transitions are numbered in accordance with Fig. 4 below.

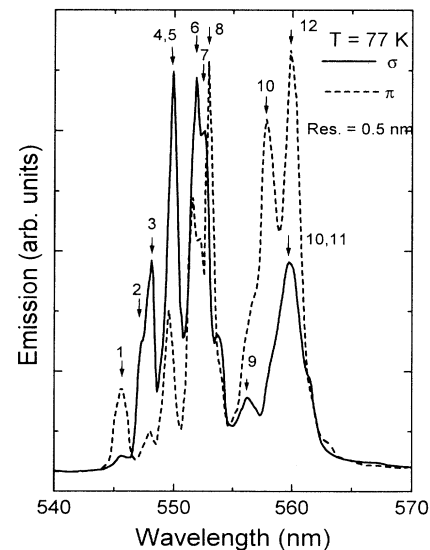


FIG. 3. Absorption spectra of $\text{LiNbO}_3:\text{Er}^{3+}$ at liquid nitrogen temperatures. Some of the lines are numbered, and are identified as transitions in Fig. 4 below.

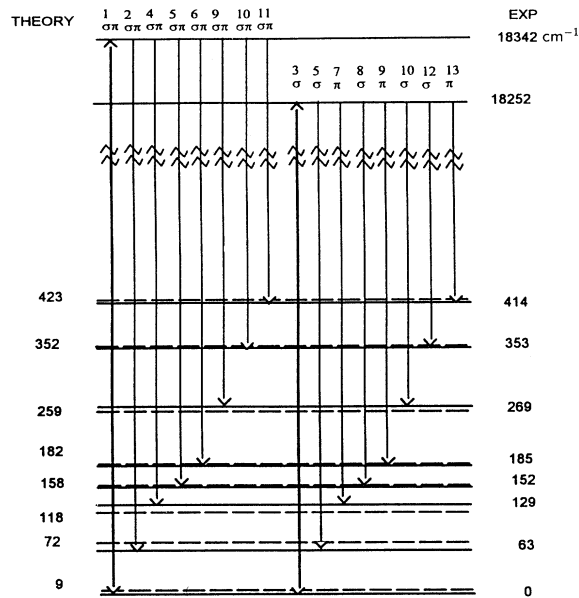


FIG. 4. Levels of $\text{LiNbO}_3:\text{Er}^{3+}$ as obtained from the analysis of the spectra of Figs. 1–3. The numbering allows one to identify the transitions observed by absorption or fluorescence. The polarization allowed is also indicated at the top of each transition.

to the $^4I_{15/2}$ experimental energies. As the number of independent parameters in the crystal-field energy, for the C_3 point symmetry and $4f$ electrons, is 7, and the number of observed levels is of the same order, we needed to make some assumptions. Looking at the crystal sites allowed for the Er^{3+} ion, we see that they can be considered as octahedral, distorted in the direction of the C_3 axis, and with, further, a small tetragonal distortion. On this basis, we wrote the first term in the right hand side

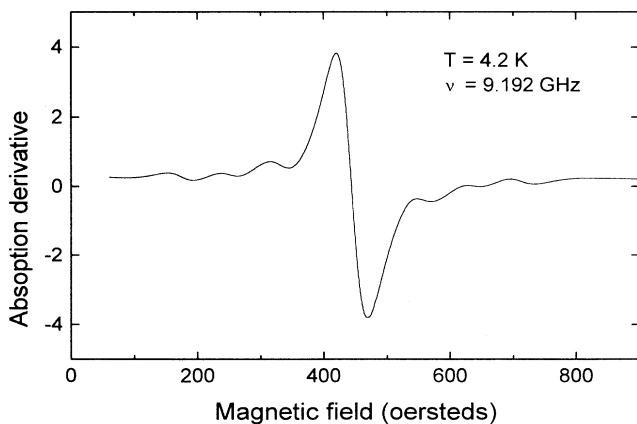


FIG. 5. The $\text{LiNbO}_3:\text{Er}^{3+}$ EPR spectrum, consisting of the lowest doublet resonance. The satellite lines are the hyperfine transitions corresponding with ^{167}Er ($I = 7/2$). The ordinate axis is in arbitrary units.

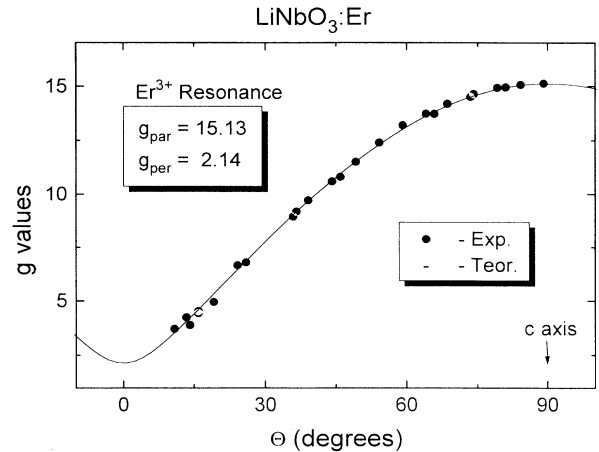


FIG. 6. Angular variation of the central line in Fig. 5. The g values obtained experimentally agree well with those corresponding with the lowest level of Fig. 4 (see text).

of Eq. (1) that corresponds to an axial distortion in the c -axis direction; the second term represents a distortion in the tetragonal direction, and the last two terms are the cubic crystal field. The $O_n^m(c)$ and $O_n^m(s)$ are Stevens' spin operators transforming as the real combinations of spherical harmonics C_n^m and S_n^m tabulated by Prather.⁸ The last two terms correspond to the cubic crystal field, and O_4 and O_6 are the fourth and sixth order cubic linear combinations of operators.⁹ We choose to write down Eq. (1) in the cubic axes, instead of the trigonal axes, for better understanding of the fitting parameters. We obtain

$$\begin{aligned} B_2^0 &= (1.30 \pm 0.05) \times 10^{-1} \text{ cm}^{-1}, \\ B_2 &= (6.51 \pm 0.05) \times 10^{-1} \text{ cm}^{-1}, \\ B_4 &= (5.21 \pm 0.08) \times 10^{-3} \text{ cm}^{-1}, \\ B_6 &= (3.75 \pm 0.10) \times 10^{-5} \text{ cm}^{-1}. \end{aligned}$$

The ESR spectra of Er^{3+} in LiNbO_3 present a single line, accompanied by the corresponding satellites of the ^{167}Er isotope, with $I = 7/2$, as can be seen in Fig. 5. The hyperfine parameter is isotropic, within the experimental error, and its value is $^{167}A = 77 \pm 3$ G. Figure 6 shows the angular variation of the isotope ^{168}Er with the magnetic field in the plane (110) of the crystal. We fit the g values of this transition by $g_{\parallel} = 15.14$ and $g_{\perp} = 2.15$. These values agree within the calculation error with that of a Kramer doublet with a wave function obtained from the diagonalization of the 16×16 crystal-field matrix of Eq. (1) for the lower $J = 15/2$ multiplet. However, the g values obtained are very much dependent on small variations in the crystal-field parameters; for this reason, the induced g shifts originating in the ferroelectricity of the crystals¹⁰ could not be evaluated.

Rutherford backscattering^{11–13} and extended x-ray-absorption fine-structure^{14,15} experiments show that the most probable site for the rare-earth impurities is the Li^+ site. The fact that the Li^+ ions are less strongly bonded to the lattice, as is shown in early x-ray diffraction experiments¹⁶ and by thermal reduction of the crystals,¹⁷

gives force to this result. XSW experiments by Gog *et al.*⁴ demonstrate, using this powerful spectroscopic technique, that the site occupied is a trigonal site near the Li site. This is completely confirmed by our experimental results, both optical and ESR. This one is a very sensitive tool to study magnetic impurities, and, as was told above, we did not find any other resonance in our samples. We cannot, from our results, define the site occupied by Er^{3+} , but we can be sure that most of the Er^{3+} ions are in only one trigonal site, as Ref. 4 demonstrates.

IV. CONCLUSIONS

Summarizing, we obtained the crystal-field parameters fitting the optical spectra of Er^{3+} in LiNbO_3 . From the calculation, we obtained the corresponding ESR g values, in good agreement with the experimental data. We observed the optical and ESR spectra corresponding to a single site for the Er^{3+} ion; we conclude that it enters in a trigonal site of the lattice, but we were not able

to decide which is the site. Gog *et al.*⁴ assert that the site occupied by Er^{3+} is that defined by them as site 1. Total energy calculations¹⁸ showed that this site is energetically favorable. We believe that this work completes previous ESR and optical studies of LiNbO_3 , and that it can help in future analysis of this system, and induce theoreticians to develop models to explain the distortion about the Er^{3+} ion. This can be useful in the future use of this system for solid state lasers or communications.

ACKNOWLEDGMENTS

The authors knowledge financial help by Fundação de Amparo à Pesquisa do Estado de São Paulo, Conselho Nacional de Pesquisas, Cordenação de Aperfeiçoamento de Pessoal do Ensino Superior e Financiadora de Estudos e Pesquisas, Brazil. We also thank João Frigo for help with the sample growing and Professor O. R. de Nascimento for suggestions about the ESR experiments.

* Permanent address: Dept. de Física, Universidade Federal de Goiás, Brazil.

¹ N.L. Evlanova, A.S. Kovalev, V.A. Koptsik, L.S. Kornienko, A.M. Prokhorov, and L.N. Rashkovich, *JETP Lett.* **5**, 291 (1967).

² G. Burns, D.F. O'Kane, and R.S. Title, *Phys. Rev.* **167**, 314 (1968).

³ B. Dischler, J.R. Herrington, A. Rauber, and J. Schneider, *Solid State Commun.* **12**, 737 (1973).

⁴ Th. Gog, M. Griebenow, and G. Materlik, *Phys. Lett. A* **181**, 417 (1993), and references therein.

⁵ L. Arizmendi and J.M. Cabrera, *Phys. Rev. B* **31**, 7138 (1985).

⁶ V.G. Grachev and G.I. Malovichko, *Sov. Phys. Solid State* **27**, 424 (1985).

⁷ R. Duchowicz, L. Nuñez, J.O. Tocho, and F. Cussó, *Solid State Commun.* **88**, 439 (1993), and references therein.

⁸ J.L. Prather, U.S. National Bureau of Standards Monograph No. 19 (U.S. GPO, Washington, DC, 1961).

⁹ K.R. Lea, M.J.M. Leask, and W.P. Wolf, *J. Phys. Chem Solids* **23**, 1381 (1962).

¹⁰ W.B. Mims, *The Linear Electric Field Effect in Paramag-*

netic Resonance (Oxford University Press, Oxford, 1976).

¹¹ L. Kovacs, L. Rebouta, J.C. Soares, and M.F. da Silva, *Radiat. Eff. Def. Solids* **119–121**, 445 (1991).

¹² L. Rebouta, J.C. Soares, M.F. da Silva, J.A. Sanz-Garcia, E. Dieguez, and F. Agullo-Lopez, *J. Mater. Res.* **7**, 130 (1992).

¹³ L. Rebouta, M.F. da Silva, J.C. Soares, J.A. Sanz-Garcia, E. Dieguez, and F. Agullo-Lopez, *Nucl. Instrum. Methods Phys. Res. Sect. B* **64**, 189 (1992).

¹⁴ C. Prieto, C. Zaldo, P. Fessler, H. Dexpert, J.A. Sanz-Garcia, and E. Dieguez, *Phys. Rev. B* **43**, 2594 (1991).

¹⁵ C. Zaldo, F. Agullo-Lopez, J. Garcia, A. Marcelli, and S. Mobilio, *Solid State Commun.* **71**, 243 (1989); C. Prieto, C. Zaldo, and J.A. Sanz-Garcia (unpublished).

¹⁶ S.C. Abrahams, J.M. Reddy, and J.L. Bernstein, *J. Phys. Chem. Solids* **27**, 997 (1966).

¹⁷ A. Garcia-Cabañez, J.A. Sanz-Garcia, J.M. Cabrera, F. Agullo-Lopez, C. Zaldo, R. Pareja, K. Polgár, K. Raksányi, and I. Fölvari, *Phys. Rev. B* **37**, 6085 (1988).

¹⁸ O.F. Schirmer, O. Theimann, and M. Wöhlecke, *J. Phys. Chem. Solids* **52**, 185 (1991); H.J. Donnersberg, S.M. Tomlinson, and C.R.A. Catlow, *ibid.* **52**, 201 (1991).